Research Article

Skin Pharmacology and Physiology

Skin Pharmacol Physiol 2020;33:30–37
DOI: 10.1159/000503262

Received: July 12, 2019
Accepted after revision: September 6, 2019
Published online: October 15, 2019

In vivo Tracking of DNA for Precise Determination of the Stratum Corneum Thickness and Superficial Microbiome Using Confocal Raman Microscopy

Jin Song Ri[a] Se Hyok Choe[a] Johannes Schleusener[b] Jürgen Lademann[b] Chun Sik Choe[a] Maxim E. Darvin[b]

[a]Kim Il Sung University, Pyongyang, Democratic People's Republic of Korea; [b]Center of Experimental and Applied Cutaneous Physiology, Department of Dermatology, Venerology and Allergology, Charité – Universitätsmedizin Berlin, Corporate Member of Freie Universität Berlin, Humboldt-Universität zu Berlin, and Berlin Institute of Health, Berlin, Germany

Keywords
Corneocytes · Keratinocytes · Cell maturation · Cell nucleus · Nucleoid · Bacteria · Skin barrier function

Abstract
The skin barrier function is mostly provided by the stratum corneum (SC), the uppermost layer of the epidermis. To noninvasively analyze the physiological properties of the skin barrier function in vivo, it is important to determine the SC thickness. Confocal Raman microscopy (CRM) is widely used for this task. In the present in vivo study, a new method based on the determination of the DNA concentration profile using CRM is introduced for determining the SC thickness. The obtained SC thickness values are compared with those obtained using other CRM-based methods determining the water and lipid depth profiles. The obtained results show almost no significant differences in SC thickness for the utilized methods. Therefore, the results indicate that it is possible to calculate the SC thickness by using the DNA profile in the fingerprint region, which is comparable with the SC thickness calculated by the water depth profiles (ANOVA test $p = 0.77$) and the lipid depth profile (ANOVA test $p = 0.74$). This provides the possibility to measure the SC thickness by using the DNA profile, in case the water or lipid profile analyses are influenced by a topically applied formulation. The increase in DNA concentration in the superficial SC (0–2 µm) is related to the DNA presence in the microbiome of the skin, which was not present in the SC depth below 4 µm.

Introduction

Since the 19th century, it has been widely accepted that the mammalian skin is provided with a skin barrier function to control the evaporation of water and to protect the organism against the penetration of exogenous substances [1]. The skin is composed of three major layers, i.e. epidermis, dermis, and hypodermis [2], and the skin barrier function is mostly ensured by the stratum corneum (SC), the uppermost layer of the epidermis [3–6]. The SC consists of 10−20 layers of corneocytes, which are enucleated flattened cells embedded in lipid lamellar regions [7–9]. The SC thickness is determined as the distance from the skin surface to the boundary between the SC and the stratum granulosum (SG) [10]; it varies according to the area and individual. The SC thickness is used to esti-

KARGER

E-Mail karger@karger.com
www.karger.com/spp

Maxim E. Darvin
Center of Experimental and Applied Cutaneous Physiology
Department of Dermatology, Venerology and Allergology
Charité – Universitätsmedizin Berlin, Charitéplatz 1, DE–10117 Berlin (Germany)
E-Mail maxim.darvin@charite.de

mate a swelling effect [11–15] in formulation-treated skin and employed for comparison of depth profiles of the lamellar and lateral organization of intercellular lipids [16, 17], water bonding state [18], concentration of natural moisturizing factor molecules [17, 19], keratin [20], and carotenoids [21, 22] in the SC. The SC thickness value is also a parameter for estimating whether the topically applied substances can overcome the skin barrier [23–27].

The SC thickness has been determined ex vivo by confocal microscopy [28], light microscopy [29], near-infrared densitometry [29, 30], and tape stripping + attenuated total reflectance-Fourier transform IR spectroscopy (ATR-FTIR) [31, 32], as well as in vivo by transepidermal water loss (TEWL) measurements/tape stripping [33] and confocal Raman microscopy (CRM) [10, 27, 34–38]. The possibility to track morphological changes of the epidermal layers visually has also been shown using two-photon tomography and laser scanning microscopy in vivo [39].

Although the infrared imaging technique is able to measure the amount of water and skin hydration, it neither provides depth-resolved information on skin hydration [40] nor the clinical in vivo applicability, because of the strong absorption of mid-infrared light by water [41, 42]. TEWL also provides valuable information on the effects of moisturizers, but almost no information about the dynamic mechanisms of the moisturizers [43], as well as depth-dependent characteristics of the permeability barrier [13, 44]. In vivo CRM is one of the few noninvasive tools to obtain full information on water concentration in the SC quantitatively [16, 45–47]. In order to calculate the SC thickness of depth-dependent CRM measurements, the water concentration profile has been analyzed using different algorithms [29, 35, 48], which was calculated from the Raman spectra in the high wavenumber (HWN, 2,000–4,000 cm^{-1}) region. Therefore, even if only the Raman spectra in the fingerprint (FP; 400–2,000 cm^{-1}) region are of interest, e.g. in order to analyze the penetration of a certain substance, the HWN spectra of the skin had to be acquired in order to determine the SC thickness. This could entail a more sophisticated experimental setup, requiring movable gratings or multiple excitation sources, and in the latter case, might induce artifacts due to varying excitation intensities in both regions. Therefore, it is desirable to determine the SC thickness based on Raman profiles in the FP region by analyzing bands specific to molecules with different characteristics in the SC than at deeper skin layers. As the corneocytes in the SC are enucleated keratinocytes, a criterion to differentiate the SC from the SG could be the DNA content.

In case of drug-induced water profile altering [11, 12, 43, 49], the methods based on the water concentration in the SC might determine the SC thickness erroneously. In these cases, the DNA-based method will be a good option for the determination of the SC thickness.

The aim of this study is to depth-dependently track the vibrational modes of DNA molecules [50] in the epidermis to determine the SC thickness in the FP region and to compare these results with the ones acquired by using the conventional water-derived SC thickness determination methods. This work also provides collective insight into the methodologies to determine the SC thickness by using CRM. Additionally, the determination of the DNA concentration in the epidermis could be useful for analyzing DNA-related diseases or the microbiome of the skin.

Materials and Methods

Volunteers

Six healthy Caucasian volunteers (3 females: 32, 45, and 62 years old, and 3 males: 23, 27, and 34 years old; average age, 37 years old) participated in this proof-of-concept study. The volunteers did not use any cosmetics on their forearms for more than 72 h and did not bath at least 4 h before the beginning of the experiments. After an acclimatization period of 20 min to the standardized laboratory conditions, skin areas of 2 × 2 cm^2 were marked on the volar forearms using a rubber barrier. Ten depth profiles were collected by using a CRM.

Confocal Raman Microscopy

The Raman spectra were acquired using a Model 3510 CRM for in vivo/ex vivo skin measurements (RiverD International B.V., Rotterdam, The Netherlands). By using two different lasers, the spectra were recorded in the FP (400–2,000 cm^{-1}, laser excitation wavelength 785 nm; power 20 mW, exposure time 5 s) and in the HWN region (2,000–4,000 cm^{-1}, laser excitation wavelength 671 nm; power 17 mW, exposure time 1 s). The Raman spectra were recorded starting 4–10 μm above the skin surface down to 30–36 μm in the skin, at 2-μm increments. The axial resolution was <5 μm and the spectral resolution was 2 cm^{-1}. The utilized CRM system has been described in detail elsewhere [10, 51, 52].

Data Analysis

For compensating the depth-dependent attenuation of the Raman signal, the area under the curve (AUC) of the Amide I band, located at 1,650 cm^{-1} in the FP region, and the keratin band, located at 2,930 cm^{-1} in the HWN region, were used as internal criteria, respectively [10, 53–55].

Determination of the Skin Surface in the FP and HWN Regions

In the FP region, the skin surface is defined as the position where the AUC of the Amide I band at 1,650 cm^{-1} reaches the half of its maximum [16]. In the HWN region, the surface of the skin is determined as the position, where the AUC of the keratin band (2,910–2,965 cm^{-1}) reaches the half of its maximum [34]. If skin is

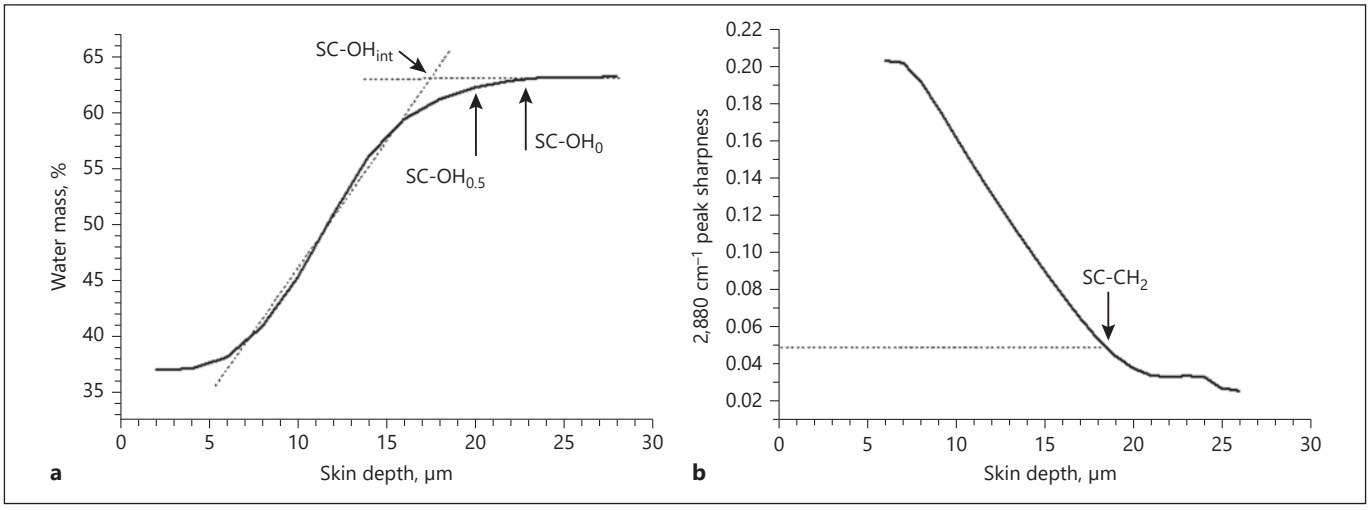

Fig. 1. The schematic of the existing methods to determine the SC thickness based on the water and lipid profiles. **a** In the water profile, the SC thickness is defined at the intersection (point SC-OH_{int}) [29] of the two dotted tangential lines in the increasing and constant region. The derivation values 0.5 and 0 are also determined as the boundary point, denoted as SC-$OH_{0.5}$ [48] and SC-OH_0 [35], respectively. **b** In the lipid profile, the position where the sharpness value is 0.05 is determined as the boundary between SC and SG (SC-CH_2) [58].

untreated, i.e. the Raman spectrum of the skin and of formulations are not overlaid, the depth profiles of both Raman peaks show similar results [55].

Determination of the SC Thickness Using the Water Profile

Normally, the water mass percentage in the SC gradually increases from the skin surface towards the SG and below, where the water concentration is maximal and constant [35, 56, 57]. Caspers et al. [10, 34] showed that the water mass percentage in the SC is proportional to the ratio of the OH vibration of water AUC (3,350–3,550 cm^{-1}) and the CH_3 vibration of protein AUC (2,910–2,965 cm^{-1}). In previous studies, three water profile-based methods to detect the boundary between the SC and the SG were applied. The first was to define it as the point where the first derivation of the water concentration reaches 0 [35]; the second was to define where it is 0.5 [48], and the third was to define it as the intersection point of two tangent lines of the increasing and almost constant regions [29]. In this study, the SC thickness was determined using these three methods abbreviated as SC-OH_0, SC-$OH_{0.5}$, and SC-OH_{int}, respectively. Figure 1a shows an exemplary water profile to illustrate the application of these methods.

Determination of SC Thickness Using the Lipid Profile

Choe et al. [58] reported that the sharpness of the lipid peak at 2,880 cm^{-1} can also be employed in determining the SC thickness. This is related to the crystallographic properties of the lipids. The sharpness of the peak at 2,880 cm^{-1} decreases towards the deeper layers of the SC and almost vanishes at the boundary between the SC and the SG. Based on our previous research, the point where the sharpness of the lipid-related Raman band at 2,880 cm^{-1} reaches a value of 0.05 could be considered as the boundary between the SC and the SG [58] (Fig. 1b). In this study, the SC thickness determined by this method was abbreviated as SC-CH_2.

Determination of the DNA Concentration

DNA exists in the nuclei of the cells. The SC consists of corneocytes, which are enucleated keratinocytes, while the SG contains nucleated keratinocytes in the last proliferation stage [59]. Therefore, the presence of DNA-related molecular vibrations was considered to indicate the boundary between the SC and the SG. The Raman bands located at 481, 678, 722, 746, 785, 828, and 1,090 cm^{-1} are related to the DNA molecules [60, 61]. It was found that the 481, 678, 722, 746, and 828 cm^{-1} bands have too small intensities, and the 1,090 cm^{-1} band is superimposed with the lipid-derived peak at 1,080 cm^{-1} [62]. Therefore, only the 785 cm^{-1} band was evaluated for further calculations (online suppl. Fig. 1a–e; see www.karger.com/doi/10.1159/000503262 for all online suppl. material). The intensity of the prominent DNA-related Raman band at 785 cm^{-1}, corresponding to O–P–O stretch vibrations of DNA [60], was examined depth-dependently. The spectral data was smoothened using a "moving average" filter. A linear baseline was drawn for the 774–800 cm^{-1} range (Fig. 2a, b). Subsequently, an AUC of the Raman bands in the 780–788 cm^{-1} range was determined. In order to compensate the depth-dependent signal attenuation of light by the skin, these AUCs were divided by that of the Amide I band (1640–1670 cm^{-1}) [17] taking the nonhomogeneous distribution of keratin in the SC into consideration [55, 63]. The detailed algorithm for the determination of the SC thickness is presented in the Results and Discussion section.

Statistical Analysis

Statistical evaluation was performed using the MATLAB R2013b software (MathWorks Inc., Natick, MA, USA). To confirm significant differences in the mean values of SC thicknesses determined by the different methods, balanced one-way ANOVA and paired *t* tests were applied. $p < 0.05$ was considered significantly different. Correlation tests were also carried out, where $p < 0.01$ was considered to be significantly correlated.

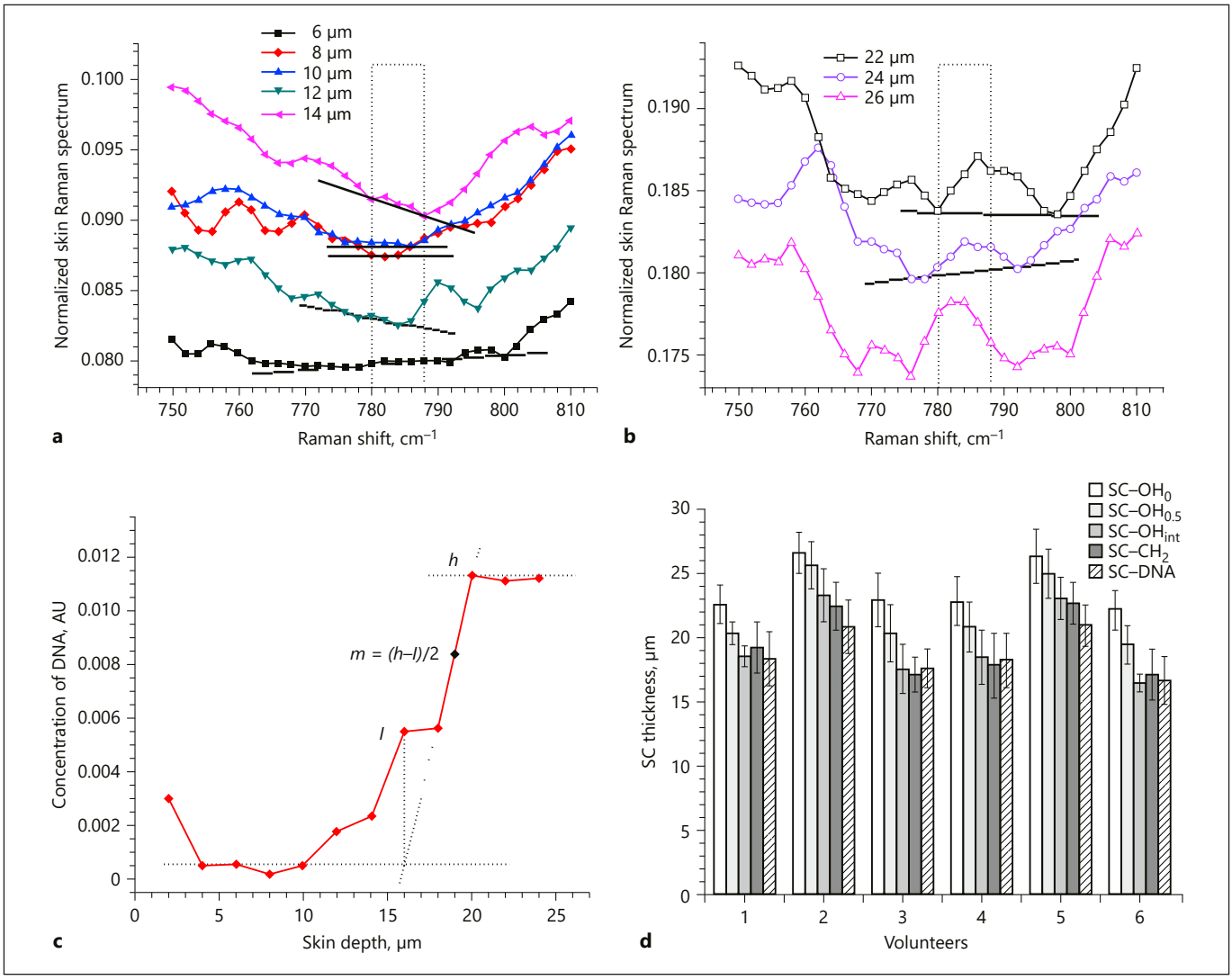

Fig. 2. Exemplary in vivo Raman spectra of one volunteer (male, 27 years old, volar forearm) in the 750–810 cm^{-1} range of skin depths of 6–14 µm (**a**) and 22–26 µm (**b**) and the corresponding depth profile of the DNA-related 785 cm^{-1} Raman band AUC (**c**), showing schematically the procedure to determine the boundary between the SC and the SG (point *h* denotes the starting point of the plateau, point *l* the point where the DNA concentration starts to increase, which is indicated by the intersection of the two dotted tangential lines, one from the constant region of the upper layers and one from the rapidly increasing region. The middle point *m* between *h* and *l*, is set as the boundary between the SC and the SG, and the SC thickness calculated by the DNA profile is denoted as SC-DNA. **d** The SC thickness values (mean ± SD for 6 volunteers) according to water, lipid, and DNA profiles.

Results and Discussion

Determination of SC Thickness by the DNA Profile

According to previous research [60, 61], the Raman bands located at 481, 678, 722, 746, 785, 828, and 1,090 cm^{-1} are related to the DNA molecules. The most prominent DNA-related Raman peak occurs at 1,090 cm^{-1} and originates from O–P–O stretching vibrations of DNA molecules. This peak is close to the lipid-derived peak at 1,080 cm^{-1} [62], which makes it difficult to separate the DNA peak from the lipid peak. The DNA peaks at 481 and 828 cm^{-1} show disordered tendencies with varying skin depths, which is probably due to the contribution of other substances. The peaks at 678, 722, and 746 cm^{-1} cannot be used to determine the SC thickness, as these intensities are too weak to be considered and are comparable with the noise levels (online suppl. Fig. 1a–e).

The strongest peak among the DNA-related Raman peaks is the peak around 785 cm^{-1}. As shown in Figure 2a, there are almost no peaks around 785 cm^{-1} in the upper layers and intermediate layers (0–14 μm), while in the deeper layers, there is a prominent peak at 785 cm^{-1} as shown in Figure 2b. Figure 2c shows the depth profile of the DNA concentration in the skin in vivo. The AUC of the peak at 785 cm^{-1} is lower and almost constant in the upper layers of the SC, which can be explained by the SC composition of enucleated cells. Near the boundary between SC and SG, it rapidly increases and remains nearly constant in the SG layer. There is a transition zone between the points marked as *l* and *h*, which implies that the disruption of keratinocytes' nuclei does not occur instantly from the SG to the SC, rather there are some remnant DNA molecules in the bottom layers of the SC. Another possible reason for the transition zone is the sampling volume of the CRM, which has a diameter of approx. 5 μm [55]. Thus, the sampling volume starts to approach the SG still being present mostly in the SC, which results in an increase in the DNA-related Raman peak intensity. Hereby, the boundary between the SC and the SG was determined as follows. Based on preliminary tests with known SC thickness values, point *h* is located deeper, and point *l*, which is the starting point of the increasing zone, is located too shallow compared with the boundary between the SC and the SG. Taking the existence of this transition zone (*h*–*l*) into consideration, the selection of the middle point (*m*) might be the most reasonable option for determining the boundary between the SC and the SG. In this study, the SC thickness determined using this procedure was abbreviated as SC-DNA.

DNA-Related Distribution of the Microbiome in the SC

The slight increase in the DNA concentration observed at the skin surface (Fig. 2c) can be explained by an influence of the microbiome of the skin, containing DNA [64]. Figure 2c shows that the microbiome has a maximal concentration in the superficial SC depths (0–2 μm) and is not present below 4 μm in healthy skin.

Determination of the SC Thickness Calculated Using CRM-Based Methods

Figure 1 shows the methods to determine the SC thickness by different criteria. As shown in Figure 1a, normally the values of the SC-OH_0 thickness are the largest, followed by the SC-$OH_{0.5}$ thickness and finally the SC-OH_{int} thickness. The difference between the SC-OH_0 and SC-$OH_{0.5}$ thickness is approx. 1.2–2.6 μm and the SC-OH_{int} thickness is approx. 3–5 μm from SC-OH_0. All of the obtained water-derived SC thickness values correlate linearly ($p < 0.01$, $R > 0.9$; Table 1). The water-, lipid- and DNA-derived SC thickness values (SC-OH_{int}, SC-CH_2, and SC-DNA) show no differences, as summarized in Figure 2d (ANOVA analysis, $p > 0.05$). This also applies to the SC thickness determined by the SC-$OH_{0.5}$, SC-CH_2, and SC-DNA methods. All correlation coefficients are >0.62 (Table 1), which indicates that the presented SC thickness values correlate linearly. The highest correlation is obtained between the SC-OH_0, SC-$OH_{0.5}$, and SC-OH_{int} groups ($R > 0.9$). The nonhomogeneity of keratin distribution in the SC [55] can potentially influence the determined water and lipid profiles used for calculating the SC thickness (Fig. 1), which can result in minor changes of the values.

Table 1. Correlation coefficients for the SC thickness values calculated using the five different methods

	SC-OH_0	SC-$OH_{0.5}$	SC-OH_{int}	SC-CH_2	SC-DNA
SC-OH_0	1	0.96	0.91	0.79	0.62
SC-$OH_{0.5}$	0.96	1	0.97	0.83	0.69
SC-OH_{int}	0.91	0.97	1	0.85	0.75
SC-CH_2	0.79	0.83	0.85	1	0.68
SC-DNA	0.62	0.69	0.75	0.68	1

As shown in Table 1, the correlations between the SC-OH_{int} and the other methods are highest. Also, the SC-$OH_{0.5}$ method shows higher correlations, which indicates that the SC-OH_{int} and SC-$OH_{0.5}$ methods are good criteria for determining the SC thickness.

Egawa et al. [35] adapted the SC-OH_0 thickness as the SC thickness without any comparison to other methods. Crowther et al. [48] used the SC-$OH_{0.5}$ thickness and compared it with results of optical coherence tomography (OCT). They revealed that the OCT-derived thickness values are 4% smaller compared to the CRM-derived thickness values, which implies that the SC thickness measured by CRM might be larger than that determined by OCT. Recently, Teixeira et al. [65] and Mahrhauser et al. [29] adapted the SC-OH_{int} thickness and compared it with near-infrared densitometry and microscopy. According to the presented results, the SC-$OH_{0.5}$ thickness has a tendency to be slightly larger than the respective values obtained using the other methods. The values determined by the SC-$OH_{0.5}$ method are about 1.8–2.4 μm larger than those determined by the SC-OH_{int} method. However, the differences are comparable with the depth resolution of the CRM. The evaluated order of determined SC thickness values using different methods is:

$SC\text{-}OH_0 > SC\text{-}OH_{0.5} \approx SC\text{-}OH_{int} = SC\text{-}CH_2 = SC\text{-}DNA$, based on the statistical significance. The SC-DNA thickness is a good option for SC thickness measurements in the FP region and also verifies that the SC has no DNA. Further, the $SC\text{-}CH_2$ thickness is a good choice in the HWN region, particularly when the range of OH vibrations (3,350–3,550 cm^{-1}) is superimposed by substance-related Raman bands or cannot be measured.

The Importance of Using Different CRM-Based Methods to Measure the SC Thicknesses

The methods for measuring the SC thickness are complementary and can be used interchangeably, when one of them cannot be applied, for example when skin is treated with water- or lipid-containing lotions or substances enforcing hydration (i.e., oils). In this case, the water profiles in the SC transform into more flat/less gradient-shaped profiles [48, 49]. This water accumulation in the SC does not easily evaporate, although the water supply is discontinued [49]. In this case, it is difficult to determine the SC thickness based on the water profiles, and the SC-DNA or $SC\text{-}CH_2$ method will serve as a good option. The proposed method could also be successfully applied when Raman spectra are measured only in the FP region without the possibility to acquire spectra in the HWN region, due to limitations of the device or to decrease the total acquisition time. The presented SC-DNA method will complement the existing methods to measure the SC thickness without the need for measurements in the HWN region. The $SC\text{-}CH_2$ method can also be used complementarily, in cases where Raman spectra are only obtained in the HWN region, e.g. to speed up the total data acquisition times, or when the water profiles cannot be calculated by enforcing hydration, i.e. excessive water accumulation [49]. The differences between the $SC\text{-}CH_2$ and the other methods can also be useful for analyzing skin diseases with lipid depletion, i.e. atopic dermatitis [66].

Conclusion

In the present study, five different methods to determine the SC thickness using CRM were investigated: three methods based on the water profile ($SC\text{-}OH_0$, $SC\text{-}OH_{0.5}$, and $SC\text{-}OH_{int}$), the lipid profile ($SC\text{-}CH_2$), and the DNA profile (SC-DNA). It was revealed that when using the water profile methods, the $SC\text{-}OH_0$ thickness was 1.2–2.6 μm larger than the $SC\text{-}OH_{0.5}$ thickness, and 3–5 μm larger than the $SC\text{-}OH_{int}$ thickness values. Meanwhile, the $SC\text{-}CH_2$ and SC-DNA thickness values were similar to the value determined by the $SC\text{-}OH_{int}$ method. The $SC\text{-}OH_{0.5}$ method is similar to the $SC\text{-}OH_{int}$ method. No significant differences were found between the SC thickness values calculated by the SC-DNA, the $SC\text{-}OH_{int}$, and the $SC\text{-}CH_2$ methods. The $SC\text{-}CH_2$ or SC-DNA methods have their own validity, based on the skin's biochemical structures. The SC-DNA method can also be used to differentiate between the normal skin and the pathologic skin with DNA mutations. Spectroscopically, it also provides new possibilities to determine the SC thickness with only Raman spectra of the FP region. The comparison between the different SC thickness determination methods reveals that the $SC\text{-}OH_{int}$ and $SC\text{-}OH_{0.5}$ methods are more reasonable than the $SC\text{-}OH_0$ method in determining the SC thickness. As a drawback, the methods based on the water profiles cannot be employed when the skin formulations, which are altering water concentration or artificially force hydration of the SC, are applied. The SC-DNA method is a good option for determining the SC thickness if the water or lipid profile is influenced or one of the methods is not applicable.

Statement of Ethics

Approval for the experiments had been obtained from the Ethics Committee of the Charité – Universitätsmedizin Berlin, and all procedures complied with the Declaration of Helsinki.

Disclosure Statement

The authors declare no conflicts of interest.

Funding Sources

J.S.R., S.H.C., and C.S.C. were supported by the National Research project of the DPR Korea for Development of the Algorithm Confocal Raman Spectra and Its Application. C.S.C. was also supported by the German Academic Exchange Service (DAAD) during his research stay at the Charité.

Author Contributions

M.E.D., J.L., and C.S.C. conceived the experiments and designed the research. C.S.C. and M.E.D. performed the research. J.S.R., S.H.C., and J.S. performed data analysis and interpretation. All authors contributed to the development of the methodology and preparation of the manuscript.

References

1 Rein H. Zur Elektrophysiologie der menschlichen Haut. Untersuchungen über Farbstoffeinwanderung in lebende Warmblüterhaut im elektrischen Felde. Z Biol. 1926;84:41–50.
2 Chilcott R, Price S, editors. Principles and Practice of Skin Toxicology. London: John Wiley & Sons; 2008.
3 Lademann J, Meinke MC, Schanzer S, Richter H, Darvin ME, Haag SF, et al. In vivo methods for the analysis of the penetration of topically applied substances in and through the skin barrier. Int J Cosmet Sci. 2012 Dec;34(6):551–9.
4 Windbergs M, Hansen S, Schroeter A, Schaefer UF, Lehr CM, Bouwstra J. From the structure of the skin barrier and dermal formulations to in vitro transport models for skin absorption: skin research in the Netherlands and in Germany. Skin Pharmacol Physiol. 2013;26(4-6):317–30.
5 Heinrich K, Heinrich U, Tronnier H. Influence of different cosmetic formulations on the human skin barrier. Skin Pharmacol Physiol. 2014;27(3):141–7.
6 van Smeden J, Janssens M, Gooris GS, Bouwstra JA. The important role of stratum corneum lipids for the cutaneous barrier function. Biochim Biophys Acta. 2014 Mar;1841(3):295–313.
7 Bouwstra JA, Ponec M. The skin barrier in healthy and diseased state. Biochim Biophys Acta. 2006 Dec;1758(12):2080–95.
8 Elias PM. Epidermal barrier function: intercellular lamellar lipid structures, origin, composition and metabolism. J Control Release. 1991;15(3):199–208.
9 Wohlrab J, Gabel A, Wolfram M, Grosse I, Neubert RH, Steinbach SC. Age- and Diabetes-Related Changes in the Free Fatty Acid Composition of the Human Stratum Corneum. Skin Pharmacol Physiol. 2018;31(6):283–91.
10 Caspers PJ, Lucassen GW, Bruining HA, Puppels GJ. Automated depth-scanning confocal Raman microspectrometer for rapid in vivo determination of water concentration profiles in human skin. J Raman Spectrosc. 2000;31(8-9):813–8.
11 Choe C, Lademann J, Darvin ME. Analysis of Human and Porcine Skin in vivo/ex vivo for Penetration of Selected Oils by Confocal Raman Microscopy. Skin Pharmacol Physiol. 2015;28(6):318–30.
12 Choe C, Schleusener J, Lademann J, Darvin ME. In vivo confocal Raman microscopic determination of depth profiles of the stratum corneum lipid organization influenced by application of various oils. J Dermatol Sci. 2017 Aug;87(2):183–91.
13 Pany A, Klang V, Brunner M, Ruthofer J, Schwarz E, Valenta C. Effect of Physical and Chemical Hair Removal Methods on Skin Barrier Function in vitro: Consequences for a Hydrophilic Model Permeant. Skin Pharmacol Physiol. 2019;32(1):8–21.
14 Abd E, Benson HA, Roberts MS, Grice JE. Follicular Penetration of Caffeine from Topically Applied Nanoemulsion Formulations Containing Penetration Enhancers: In vitro Human Skin Studies. Skin Pharmacol Physiol. 2018;31(5):252–60.
15 Stamatas GN, de Sterke J, Hauser M, von Stetten O, van der Pol A. Lipid uptake and skin occlusion following topical application of oils on adult and infant skin. J Dermatol Sci. 2008 May;50(2):135–42.
16 Choe C, Lademann J, Darvin ME. A depth-dependent profile of the lipid conformation and lateral packing order of the stratum corneum in vivo measured using Raman microscopy. Analyst (Lond). 2016 Mar;141(6):1981–7.
17 Choe C, Schleusener J, Lademann J, Darvin ME. Human skin in vivo has a higher skin barrier function than porcine skin ex vivo-comprehensive Raman microscopic study of the stratum corneum. J Biophotonics. 2018 Jun;11(6):e201700355.
18 Choe C, Lademann J, Darvin ME. Depth profiles of hydrogen bound water molecule types and their relation to lipid and protein interaction in the human stratum corneum in vivo. Analyst (Lond). 2016 Nov;141(22):6329–37.
19 Koppes SA, Kemperman P, Van Tilburg I, Calkoen-Kwa F, Engebretsen KA, Puppels GJ, et al. Determination of natural moisturizing factors in the skin: raman microspectroscopy versus HPLC. Biomarkers. 2017 Sep;22(6):502–7.
20 Choe C, Schleusener J, Lademann J, Darvin ME. Keratin-water-NMF interaction as a three layer model in the human stratum corneum using in vivo confocal Raman microscopy. Sci Rep. 2017 Nov;7(1):15900.
21 Lademann J, Caspers PJ, van der Pol A, Richter H, Patzelt A, Zastrow L, et al. In vivo Raman spectroscopy detects increased epidermal antioxidative potential with topically applied carotenoids. Laser Phys Lett. 2009;6(1):76–9.
22 Choe C, Ri J, Schleusener J, Lademann J, Darvin ME. The non-homogenous distribution and aggregation of carotenoids in the stratum corneum correlates with the organization of intercellular lipids in vivo. Exp Dermatol. 2019 Aug;exd.14018. doi: 10.1111/exd.14018. [Epub ahead of print].
23 Alonso C, Carrer V, Barba C, Coderch L. Caffeine delivery in porcine skin: a confocal Raman study. Arch Dermatol Res. 2018 Oct;310(8):657–64.
24 Laing S, Bielfeldt S, Wilhelm K-P, Obst J: Confocal Raman Spectroscopy as a tool to measure the prevention of skin penetration by a specifically designed topical medical device. Skin Res Technol. 2019 Jul;25(4):578-586.
25 Tippavajhala VK, de Oliveira Mendes T, Martin AA. In Vivo Human Skin Penetration Study of Sunscreens by Confocal Raman Spectroscopy. AAPS PharmSciTech. 2018 Feb;19(2):753–60.
26 Czekalla C, Schönborn KH, Lademann J, Meinke MC. Noninvasive Determination of Epidermal and Stratum Corneum Thickness in vivo Using Two-Photon Microscopy and Optical Coherence Tomography: Impact of Body Area, Age, and Gender. Skin Pharmacol Physiol. 2019;32(3):142–50.
27 Zhang Z, Lunter DJ. Confocal Raman microspectroscopy as an alternative to differential scanning calorimetry to detect the impact of emulsifiers and formulations on stratum corneum lipid conformation. Eur J Pharm Sci. 2018 Aug;121:1–8.
28 Moghadam SH, Saliaj E, Wettig SD, Dong C, Ivanova MV, Huzil JT, et al. Effect of chemical permeation enhancers on stratum corneum barrier lipid organizational structure and interferon alpha permeability. Mol Pharm. 2013 Jun;10(6):2248–60.
29 Mahrhauser DS, Nagelreiter C, Gehrig S, Geyer A, Ogris M, Kwizda K, et al. Assessment of Raman spectroscopy as a fast and non-invasive method for total stratum corneum thickness determination of pig skin. Int J Pharm. 2015 Nov;495(1):482–4.
30 Egawa M, Yanai M, Maruyama N, Fukaya Y, Hirao T. Visualization of Water Distribution in the Facial Epidermal Layers of Skin Using High-Sensitivity Near-Infrared (NIR) Imaging. Appl Spectrosc. 2015 Apr;69(4):481–7.
31 Greve TM, Andersen KB, Nielsen OF. ATR-FTIR, FT-NIR and near-FT-Raman spectroscopic studies of molecular composition in human skin in vivo and pig ear skin in vitro. Spectroscopy (Springf). 2008;22:437-57.
32 Rawlings AV. Molecular basis for stratum corneum maturation and moisturization. Br J Dermatol. 2014 Sep;171 Suppl 3:19–28.
33 Sekkat N, Kalia YN, Guy RH. Biophysical study of porcine ear skin in vitro and its comparison to human skin in vivo. J Pharm Sci. 2002 Nov;91(11):2376–81.
34 Caspers PJ, Lucassen GW, Carter EA, Bruining HA, Puppels GJ. In vivo confocal Raman microspectroscopy of the skin: noninvasive determination of molecular concentration profiles. J Invest Dermatol. 2001 Mar;116(3):434–42.
35 Egawa M, Hirao T, Takahashi M. In vivo estimation of stratum corneum thickness from water concentration profiles obtained with Raman spectroscopy. Acta Derm Venereol. 2007;87(1):4–8.
36 Bielfeldt S, Schoder V, Ely U, Van Der Pol A, De Sterke J, Wilhelm KP. Assessment of human stratum corneum thickness and its barrier properties by in-vivo confocal Raman spectroscopy. Int J Cosmet Sci. 2009;31(6):479–80.
37 Bouwstra JA, de Graaff A, Gooris GS, Nijsse J, Wiechers JW, van Aelst AC. Water distribution and related morphology in human stratum corneum at different hydration levels. J Invest Dermatol. 2003 May;120(5):750–8.

38 Choe C, Schleusener J, Lademann J, Darvin ME. Age related depth profiles of human Stratum Corneum barrier-related molecular parameters by confocal Raman microscopy in vivo. Mech Ageing Dev. 2018 Jun;172:6–12.
39 Darvin ME, Richter H, Zhu YJ, Meinke MC, Knorr F, Gonchukov SA, et al. Comparison of in vivo and ex vivo laser scanning microscopy and multiphoton tomography application for human and porcine skin imaging. Quantum Electron. 2014;44(7):646–51.
40 Zhang SL, Meyers CL, Subramanyan K, Hancewicz TM. Near infrared imaging for measuring and visualizing skin hydration. A comparison with visual assessment and electrical methods. J Biomed Opt. 2005 May-Jun;10(3):031107.
41 Kikuchi S, Aosaki T, Bito K, Naito S, Katayama Y. In vivo evaluation of lateral lipid chain packing in human stratum corneum. Skin Res Technol. 2015 Feb;21(1):76–83.
42 Kendall C, Isabelle M, Bazant-Hegemark F, Hutchings J, Orr L, Babrah J, et al. Vibrational spectroscopy: a clinical tool for cancer diagnostics. Analyst (Lond). 2009 Jun;134(6):1029–45.
43 Caussin J, Groenink HW, de Graaff AM, Gooris GS, Wiechers JW, van Aelst AC, et al. Lipophilic and hydrophilic moisturizers show different actions on human skin as revealed by cryo scanning electron microscopy. Exp Dermatol. 2007 Nov;16(11):891–8.
44 van Logtestijn MD, Domínguez-Hüttinger E, Stamatas GN, Tanaka RJ. Resistance to water diffusion in the stratum corneum is depth-dependent. PLoS One. 2015 Feb;10(2):e0117292.
45 Falcone D, Uzunbajakava NE, Varghese B, de Aquino Santos GR, Richters RJ, van de Kerkhof PC, et al. Microspectroscopic Confocal Raman and Macroscopic Biophysical Measurements in the in vivo Assessment of the Skin Barrier: Perspective for Dermatology and Cosmetic Sciences. Skin Pharmacol Physiol. 2015;28(6):307–17.
46 Mujica Ascencio S, Choe C, Meinke MC, Müller RH, Maksimov GV, Wigger-Alberti W, et al. Confocal Raman microscopy and multivariate statistical analysis for determination of different penetration abilities of caffeine and propylene glycol applied simultaneously in a mixture on porcine skin ex vivo. Eur J Pharm Biopharm. 2016 Jul;104:51–8.
47 Kourkoumelis N, Balatsoukas I, Moulia V, Elka A, Gaitanis G, Bassukas ID. Advances in the in Vivo Raman Spectroscopy of Malignant Skin Tumors Using Portable Instrumentation. Int J Mol Sci. 2015 Jun;16(7):14554–70.
48 Crowther JM, Sieg A, Blenkiron P, Marcott C, Matts PJ, Kaczvinsky JR, et al. Measuring the effects of topical moisturizers on changes in stratum corneum thickness, water gradients and hydration in vivo. Br J Dermatol. 2008 Sep;159(3):567–77.
49 Egawa M, Tagami H. Comparison of the depth profiles of water and water-binding substances in the stratum corneum determined in vivo by Raman spectroscopy between the cheek and volar forearm skin: effects of age, seasonal changes and artificial forced hydration. Br J Dermatol. 2008 Feb;158(2):251–60.
50 Painsi C, Hesterberg K, Lademann J, Knorr D, Patzelt A, Vandersee S, et al. Influence of Storage and Preservation Techniques on Egg-Derived Carotenoids: A Substantial Source for Cutaneous Antioxidants. Skin Pharmacol Physiol. 2019;32(2):65–71.
51 Darvin ME, Meinke MC, Sterry W, Lademann J. Optical methods for noninvasive determination of carotenoids in human and animal skin. J Biomed Opt. 2013 Jun;18(6):61230.
52 Zhu Y, Choe CS, Ahlberg S, Meinke MC, Alexiev U, Lademann J, et al. Penetration of silver nanoparticles into porcine skin ex vivo using fluorescence lifetime imaging microscopy, Raman microscopy, and surface-enhanced Raman scattering microscopy. J Biomed Opt. 2015 May;20(5):051006.
53 Boireau-Adamezyk E, Baillet-Guffroy A, Stamatas GN. Age-dependent changes in stratum corneum barrier function. Skin Res Technol. 2014 Nov;20(4):409–15.
54 Tfayli A, Guillard E, Manfait M, Baillet-Guffroy A. Raman spectroscopy: feasibility of in vivo survey of stratum corneum lipids, effect of natural aging. Eur J Dermatol. 2012 Jan-Feb;22(1):36–41.
55 Choe C, Choe S, Schleusener J, Lademann J, Darvin ME. Modified normalization method in in vivo stratum corneum analysis using confocal Raman microscopy to compensate nonhomogeneous distribution of keratin. J Raman Spectrosc. 2019;50:945–57.
56 Warner RR, Myers MC, Taylor DA. Electron probe analysis of human skin: determination of the water concentration profile. J Invest Dermatol. 1988 Feb;90(2):218–24.
57 Sdobnov AY, Darvin ME, Schleusener J, Lademann J, Tuchin VV. Hydrogen bound water profiles in the skin influenced by optical clearing molecular agents-Quantitative analysis using confocal Raman microscopy. J Biophotonics. 2019 May;12(5):e201800283.
58 Choe C, Lademann J, Darvin ME. Lipid organization and stratum corneum thickness determined in vivo in human skin analyzing lipid–keratin peak (2820–3030 cm−1) using confocal Raman microscopy. J Raman Spectrosc. 2016;47(11):1327–31.
59 Zhang G, Moore DJ, Flach CR, Mendelsohn R. Vibrational microscopy and imaging of skin: from single cells to intact tissue. Anal Bioanal Chem. 2007 Mar;387(5):1591–9.
60 Movasaghi Z, Rehman S, Rehman IU. Raman Spectroscopy of Biological Tissues. Appl Spectrosc Rev. 2007;42(5):493–541.
61 Bankapur A, Krishnamurthy RS, Zachariah E, Santhosh C, Chougule B, Praveen B, et al. Micro-Raman spectroscopy of silver nanoparticle induced stress on optically-trapped stem cells. PLoS One. 2012;7(4):e35075.
62 Vyumvuhore R, Tfayli A, Duplan H, Delalleau A, Manfait M, Baillet-Guffroy A. Effects of atmospheric relative humidity on Stratum Corneum structure at the molecular level: ex vivo Raman spectroscopy analysis. Analyst (Lond). 2013 Jul;138(14):4103–11.
63 Darvin ME, Choe CS, Schleusener J, Lademann J. Non-invasive depth profiling of the stratum corneum in vivo using confocal Raman microscopy considering the non-homogeneous distribution of keratin. Biomed Opt Express. 2019 May;10(6):3092–103.
64 Byrd AL, Belkaid Y, Segre JA. The human skin microbiome. Nat Rev Microbiol. 2018 Mar;16(3):143–55.
65 Teixeira AP, Rangel JL, Raniero LJ, Tosato MG, Fávero PP, Martin AA. Confocal Raman spectroscopy: determination of natural moisturizing factor profile related to skin hydration. Rev Bras Eng Biomed. 2014;30:11–16.
66 Zhang L, Cambron T, Niu Y, Xu Z, Su N, Zheng H, et al. MCR Approach Revealing Protein, Water, and Lipid Depth Profile in Atopic Dermatitis Patients' Stratum Corneum via in Vivo Confocal Raman Spectroscopy. Anal Chem. 2019 Feb;91(4):2784–90.